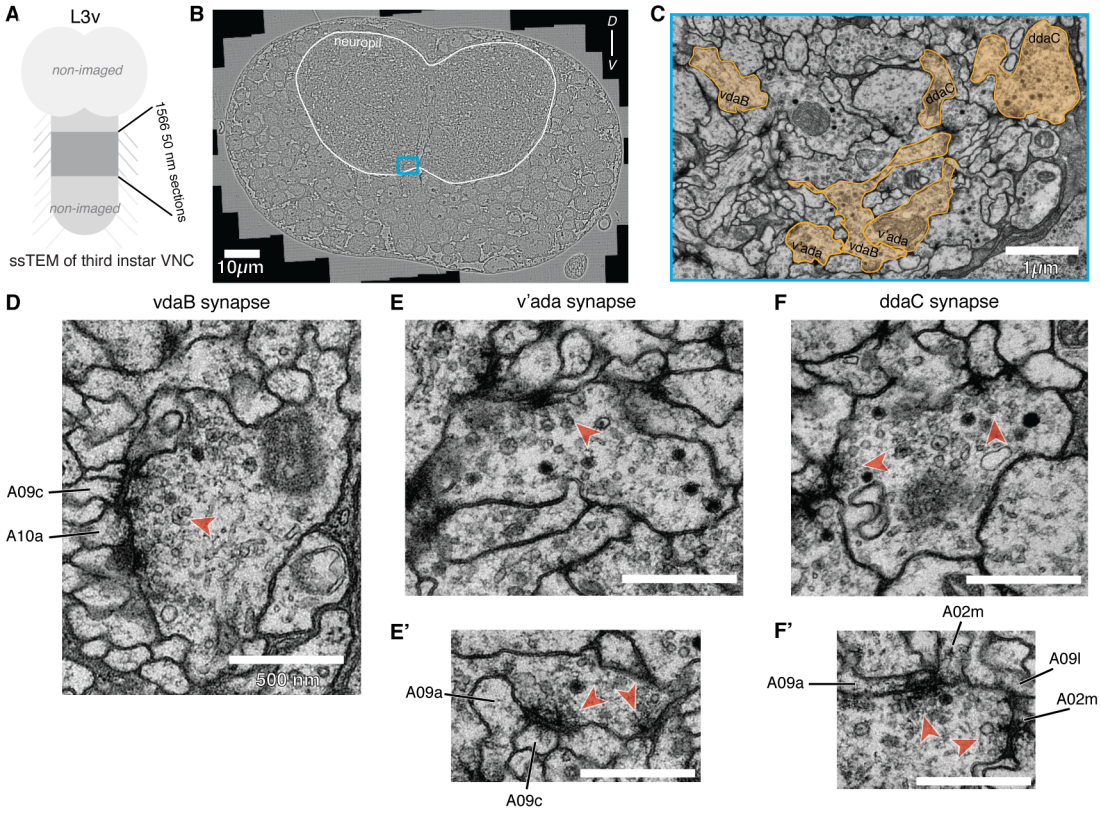

Figure 1—figure supplement 1: **A new EM image volume of a 3rd instar larva ventral nerve cord. A**, Schematic of the region of the 3rd instar larva CNS sectioned and imaged for the L3v. Anterior is up. **B**, A single section of L3v includes the complete neuropil (region inside white outline) and all soma (region outside white outline). Dorsal is up. **C**, Ventromedial neuropile indicated in the blue outline in **B**. Neurite cross-sections highlighted in orange correspond to ipsilateral mdIV axons. **D–F'**, Example synapses from vdaB (**E**), v'ada (**E,E'**), and ddaC (**F,F'**) terminals. Vesicles and presynaptic specializations highlighted by the red arrowhead. Postsynaptic neurons from LNs described in the main text are highlighted. Note the combination of small and dense core vesicles found in all three mdIV neurons.

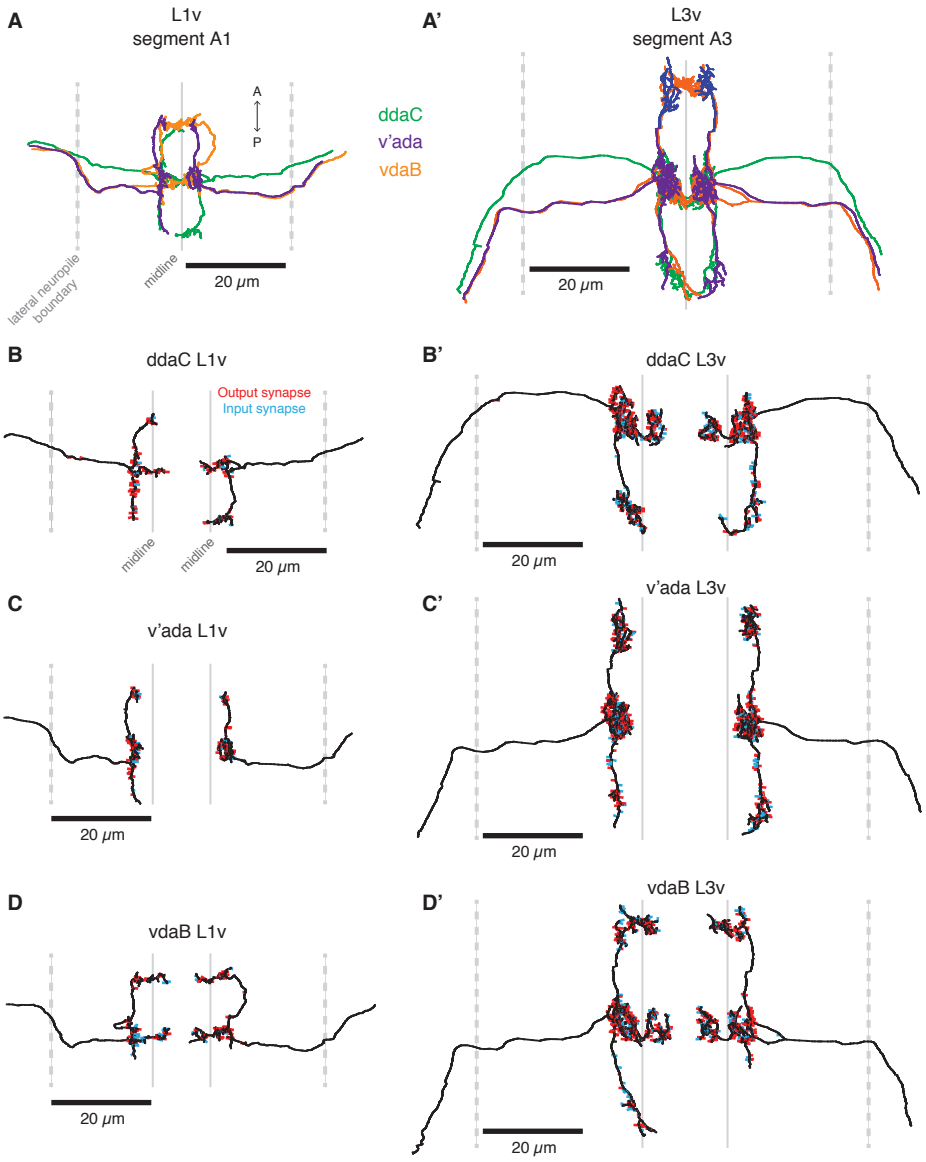

Figure 1—figure supplement 2: **Reconstructions of mdIV terminals. A, A'**, Dorsal view of all mdIV terminals from the L1v (**A**) and L3v (**A'**), identities as labeled. Views are at the same scale. Dashed lines indicate lateral neuropil boundaries, solid line the midline. **B, B'**, ddaC terminals in the L1v (**B**) and L3v (**B'**), left and right shown separately for clarity, as in all subsequent panels. ddaC can be distinguished by a midline crossing where the axon initially approaches the midline from the nerve and a projection into the adjacent segment posterior with little to no midline crossing. **C, C'**, v'ada terminals in the L1v ((**C**) and L3v (**C'**) can be distinguished by a lack of midline crossings and a consistent projection into the adjacent segments anterior and, typically, posterior. **D, D'**, vdaB terminals in the L1v ((**D**) and L3v (**D'**) can be distinguished by a midline crossing both where the axon initially approaches the midline and a second midline crossing in the adjacent segment anterior. Note that for all mdIV types, there is some variability — extra and missing branches, such as the right L1v v'ada, are true reflections of the data — although one form is more typical than others.

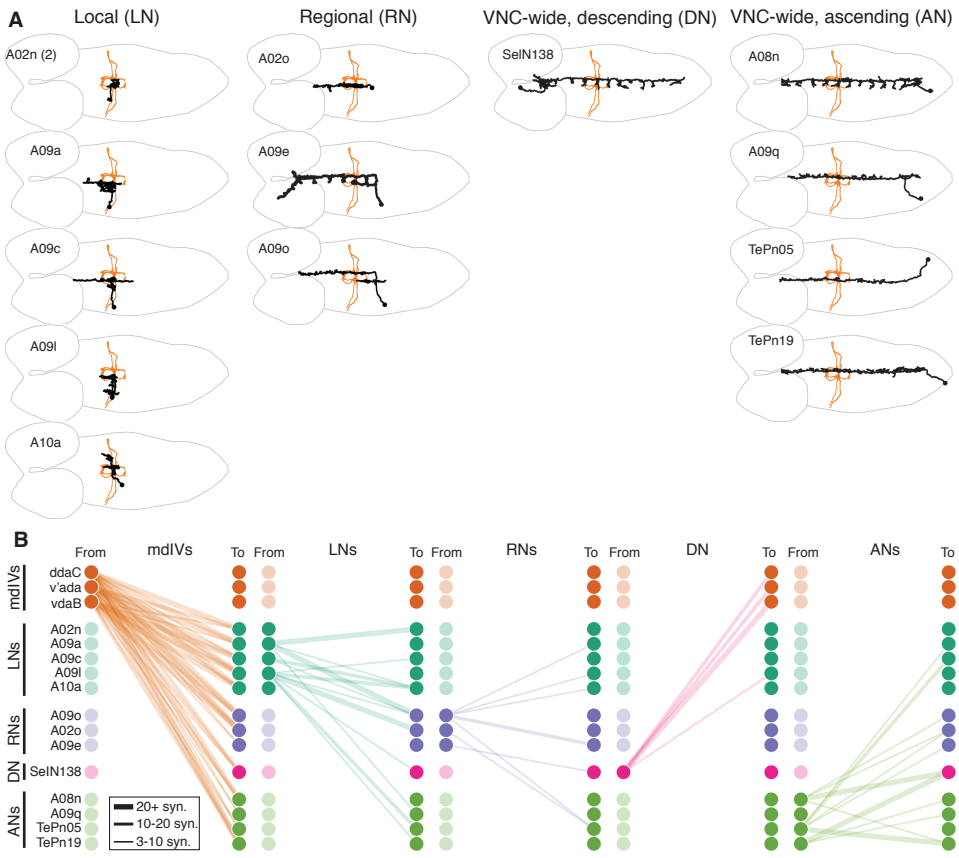

Figure 2—figure supplement 1: **The complete mdIV-connected network from the L1v. A**, All cell types synaptically connected to mdIV terminals in the L1v. Cell types were organized by spatial extent of the dendrites. Dorsal views of a single example of each interneuron cell type (black) and the mdIV terminals of segment A1 (orange), anterior to left. Outline indicates CNS boundary. Local neurons (LNs) had dendrites spanning 1-2 segments, Regional neurons (RNs) had dendrites spanning 3+ segments but not the whole VNC, a Descending neuron (DN) had dendrites in subesophageal zone (SEZ) and an axon in VNC, and Ascending neurons (ANs) had cell bodies in the posterior tip and projections that spanned the entire VNC toward the brain. See Supplemental Atlas for more views of cell types. **B**, Connectivity between cell types in the mdIV network. Each column indicates connections from cell types in the left category to all cell types. Line thickness indicates number of synapses. Connections not observed at least twice at a 3+ synapse level are not shown here. In addition to the LN networks discussed elsewhere, we also find a strong pathway for feedback regulation of mdIV terminals. The SEZ neuron SeIN138 has an axonal projection descending through every abdominal segment, along which it both receives synaptic input from and outputs back onto mdIV terminals of all subtypes, offering a local axo-axonal feedback pathway across just a few microns of axonal arbor. Interestingly, SeIN136 also receives dendritic input near the SEZ from two ascending mdIV projection neurons, A08m and TePn19, that receive mdIV input throughout the nerve cord. This mdIV→AN→DN→mdIV pathway could allow every mdIV terminal across the body to be presynaptically regulated by ascending nociceptive input coming from any one location on the body. No other cell type was strongly or consistently presynaptic to mdIV terminals, suggesting this is the only such direct pathway.

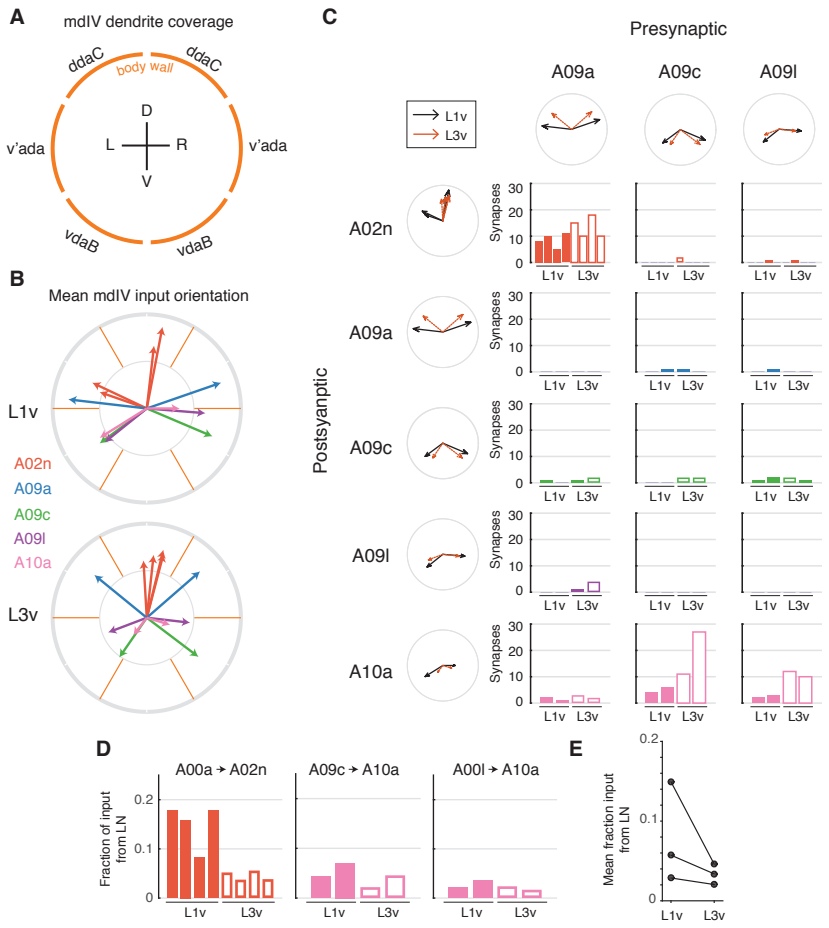

Figure 2—figure supplement 2: **Topographically structured connectivity onto and between mdIV-related LNs**. **A**, Cross-sectional schematic indicating approximate spatial receptive fields of mdIV dendrites on the body wall. View from posterior. **B**, Average orientation vector of synaptic input into LNs in the L1v (top) and L3v (bottom) for each LN (arrows). Each mdIV terminal was associated with a unit vector $\pi/3$ radians apart (orange lines, oriented toward the center of each mdIV dendritic fields). The input orientation vector for each LN is the synapse-count-weighted average of its input from mdIVs. The gray circle corresponds to a maximally specific receptive field, *i.e.* if all synapses came from a single mdIV neuron. **C**, Connectivity between LN cell types in the L1v (solid bars) and L3v (empty bars). LN cell type columns and rows are shown with spatial receptive fields from **B**. Each cell type that was strongly connected in the L1v was again connected in the L3v. Interestingly, the dorsally oriented A09a targeted the dorsally oriented A02n and the ventrolaterally oriented A09c and A09l targeted the ventrolaterally oriented A10a, suggesting feed-forward topographic microcircuits. **D**, Synaptic connectivity between LNs, normalized by total number of dendritic input synapses of the postsynaptic neuron. **E**, Mean strength, measured as fraction of total synaptic inputs, for specific connections between cell types in the L1v and L3v. The number of data points is too small to make a statistical conclusion.

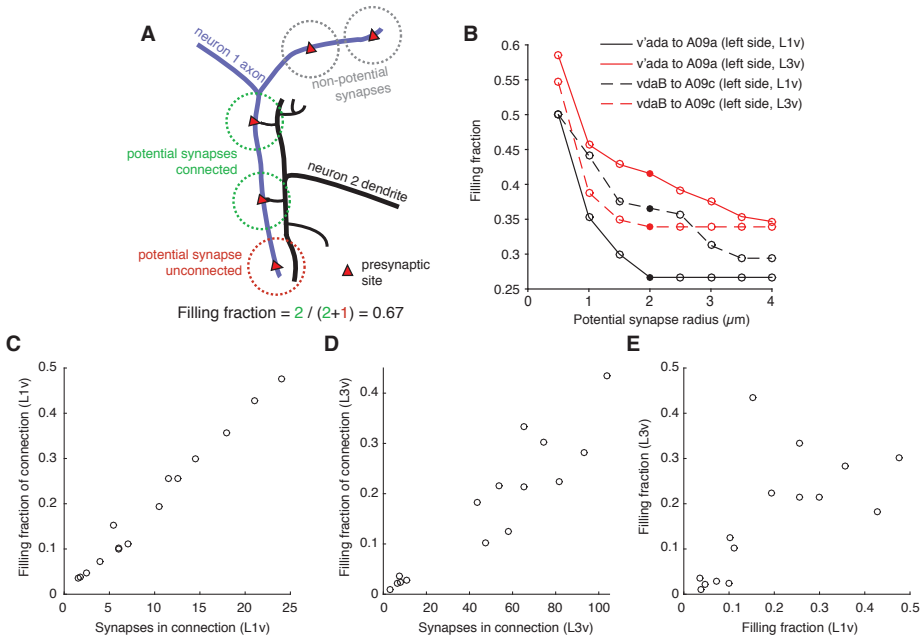

Figure 2—figure supplement 3: **Filling fraction as a measure of connection strength.** **A**, Cartoon describing the filling fraction for a connection from Neuron 1 (purple) to Neuron 2 (black). Neurons can only be connected where they are adjacent to one another in space. Because of developmental variations in arbor size and shape (see Figure 1–figure supplement 2 for variability in mdIV axon terminals), the number of regions of adjacency between a given pair of neurons can differ considerably. The concept of filling fraction [32] accounts for this type of variability by computing what fraction of potential synapses, *i.e.* those synapses spatially close enough to be connected, are actually connected. Here, we define a potential synapse from neuron 1 to neuron 2 to be those presynaptic sites on neuron 1 for which a neurite from neuron 2 passes within a given radius (dashed circles). Filling fraction is then the number of potential synapses (red and green dashed circles) that are truly connected (green dashed circles only). Note that this slightly differs from the original definition in that the version used here only observed presynaptic sites, not any location on the axon. This change was made for two reasons: 1) Synaptic regions on mdIV terminals are highly clustered with regions that typically have no presynaptic sites, and 2) Dendrites and axons are frequently co-linear in *Drosophila*, such that potential synapses would not be punctuate, as they were in the light-microscopy mammalian data analyzed using the original definition. **B**, Dependence of filling fraction on the potential synapse radius (*i.e.* the radius of the dashed grey circles in **A**) for four example connections. As the radius increases, the number of potential synapses increases and thus the filling fraction decreases. We chose 2 μm (filled circles) as a compromise between the typical size of a terminal branch and a shoulder in the filling-fraction versus radius curve. **C–D**, Mean filling fraction vs. mean number of synapses for connections between mdIV types onto LN types for the L1v (**C**) and L3v (**D**). Each data point represents one postsynaptic neuron and its input from a single mdIV subtype (vdaB, v'ada, or ddaC, left and right axons combined). The high correlation in both the L1v (Pearson r = 0.99) and L3v (Pearson r = 0.93) suggests that increased connection probability, not merely access to differing numbers of presynaptic synapses, sets synaptic specificity and connection weight. **E**, Relationship between filling fraction in the L1v and L3v are correlated (Pearson r = 0.64), suggesting that filling fraction is well conserved between individuals and across larval development.

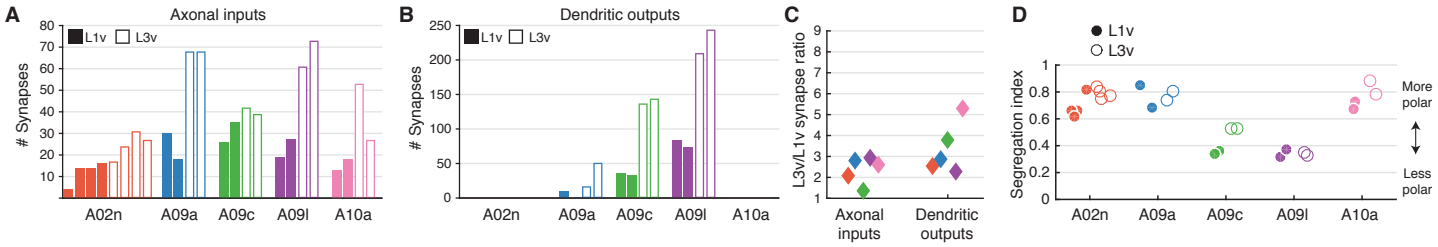

Figure 2—figure supplement 4: **Additional LN properties. A**, Number of synaptic inputs on axons of each LN. **B**, Number of synaptic outputs on dendrites of each LN. **C**, Fold-change in total axonal inputs and dendritic outputs for LN cell types between the L1v and L3v. Colors correspond to cell types. **D**, Segregation index for all LNs, a measure of the degree of input/output segregation of a neuron (1 indicates a completely segregated neuron, with all outputs in one region and all inputs in another; 0 indicated a neuron with completely intermixed inputs and outputs. See [25] for details). Note that segregation index is generally maintained as a cell-type specific property across larval stages.

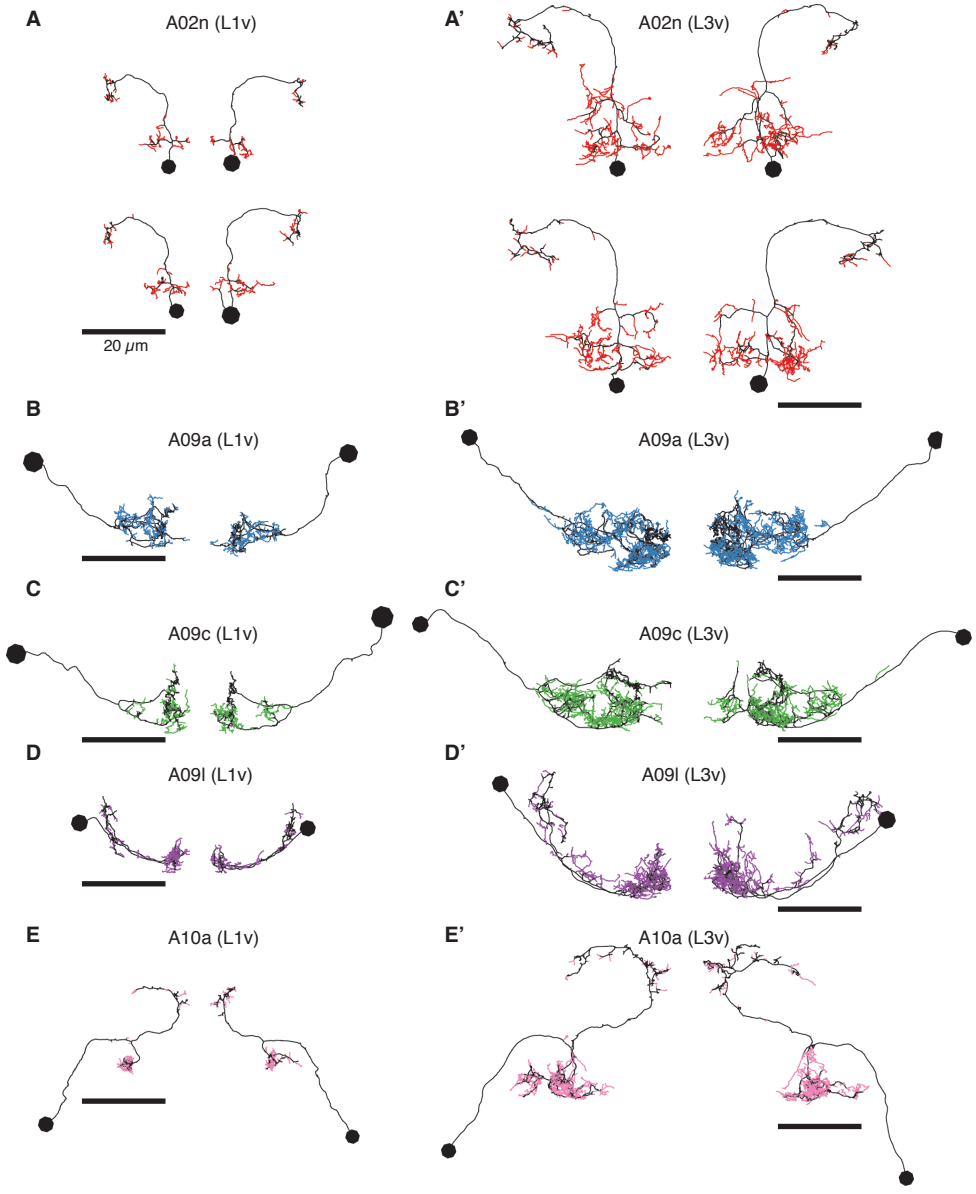

Figure 3—figure supplement 1: **Twig and backbone breakdown for all LNs.** Backbones are shown in black, twigs with colors. Neurons from the L1v are shown to left (Regular letters), neurons from the L3v to right (Primed letters). Posterior view with dorsal up. Scales are consistent across all figures, scale bars are 20 μm.

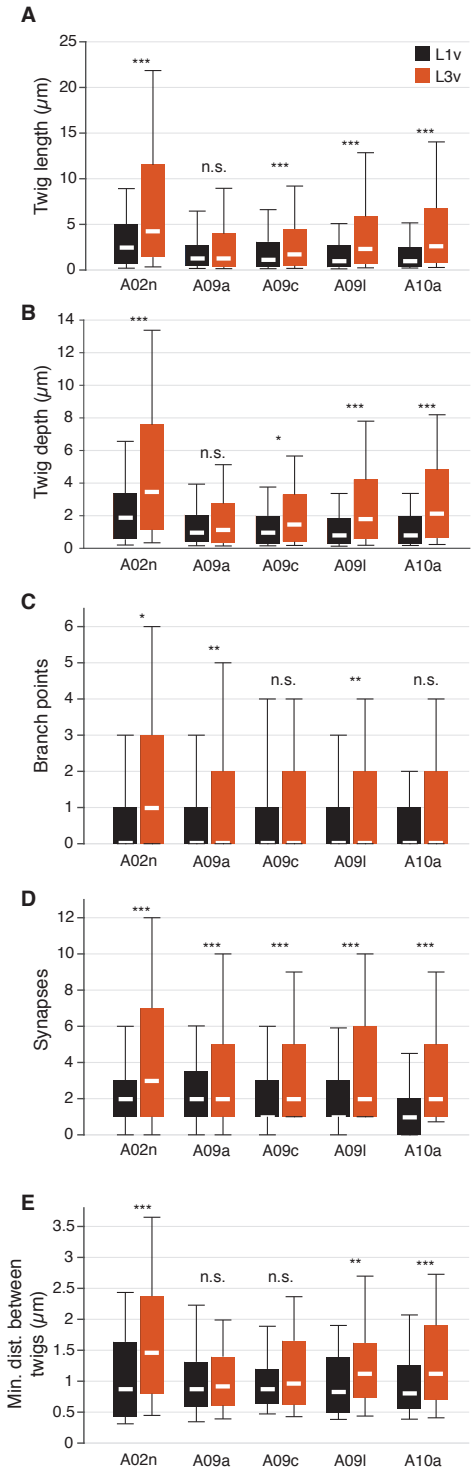

Figure 4—figure supplement 1: **Individual twig properties, broken down by LN cell type.** For each panel, bars indicate interquartile intervals, whiskers show 5/95 percentile lines. White dashes indicate median. Each bar describes two cells (four for A02n), and each twig was weighted equally. **A,** Box plots of total cable length per twig by cell type and developmental stage. **B,** Box plots of maximum twig depth (distance from distal tip to twig base) by cell type and developmental stage. **C,** Box plots of number of brach points per twig by cell type and developmental stage. **D,** Box plots of number of input synapses per twig by cell type and developmental stage. **C,** Box plots of minimum distance between twig bases along neuronal backbone by cell type and developmental stage. *: $p<0.05$, **: $p<0.01$, ***: $p<0.001$, n.s.: not significant, two-sided t-test with Bonferonni correction.

Supplemental Atlas : **Atlas of all cell types synaptically connected to mdIVs.** For each cell type, we show a dorsal view (with CNS boundary, anterior up), a sagittal view (anterior to right), a cross-sectional view (grey line indicates neuropile boundary), and a table of number and fraction (in parentheses) of synapses from mdIV neurons onto the neuron shown. Due to varying anteroposterior extents of neurons, sagittal views are not to scale.